

AD-A105 110

STANFORD UNIV CA EDWARD L GINZTON LAB OF PHYSICS F/G 20/3
ELASTIC DOMAIN WALL WAVES IN FERROELECTRIC CERAMICS AND SINGLE CRYSTALS
SEP 81 B A AULD N00014-79-C-0222
6L-3314 NL

UNCLASSIFIED

1 of 1
AS
308 10



END

DATE

FILED

10-81

DTIC

AD A105110

(12)
ELASTIC DOMAIN WALL WAVES IN FERROELECTRIC
CERAMICS AND SINGLE CRYSTALS

Annual Progress Report.

1 February 1980 - 31 January 1981

Contract No. N00014-79-C-0222 ✓

14
G.L. Report No. 3314

11 September 1981

DTIC
ELECTE
OCT 5 1981
A

Principal Investigator

B. A. Auld

This document has been approved
for public release and sale; its
distribution is unlimited.

Edward L. Ginzton Laboratory
W. W. Hansen Laboratories of Physics
Stanford University
Stanford, California 94305

DTIC FILE COPY

REPORT DOCUMENTATION PAGE		READ INSTRUCTIONS BEFORE COMPLETING FORM
1. REPORT NUMBER	2. GOVT ACCESSION NO. AD-A105110	3. RECIPIENT'S CATALOG NUMBER
4. TITLE (and Subtitle) ELASTIC DOMAIN WALL WAVES IN FERROELECTRIC CERAMICS AND SINGLE CRYSTALS		5. TYPE OF REPORT & PERIOD COVERED Annual Progress Report 1 Feb. 1980 - 31 Jan. 1981
7. AUTHOR(s) B. A. Auld		6. PERFORMING ORG. REPORT NUMBER G.L. Report No. 33140
9. PERFORMING ORGANIZATION NAME AND ADDRESS Edward L. Ginzton Laboratory W. W. Hansen Laboratories of Physics Stanford University, Stanford, CA 94305		8. CONTRACT OR GRANT NUMBER(s) N00014-79-C-0222
11. CONTROLLING OFFICE NAME AND ADDRESS Director, Metallurgy and Ceramics Program Office of Naval Research 800 N. Quincy St., Arlington, VA 22217		10. PROGRAM ELEMENT, PROJECT, TASK AREA & WORK UNIT NUMBERS
14. MONITORING AGENCY NAME & ADDRESS (if different from Controlling Office)		12. REPORT DATE September 1981
		13. NUMBER OF PAGES 24
		15. SECURITY CLASS. (of this report) UNCLASSIFIED
		15a. DECLASSIFICATION/DOWNGRADING SCHEDULE
16. DISTRIBUTION STATEMENT (of this Report) Approved for Public Release -- Distribution Unlimited		
17. DISTRIBUTION STATEMENT (of the abstract entered in Block 20, if different from Report)		
18. SUPPLEMENTARY NOTES		
19. KEY WORDS (Continue on reverse side if necessary and identify by block number) Piezoelectricity Guided Waves Electrostriction Elastic Waveguides Domain Walls Elastic Attenuation Counter Poling Laser Probing Ferroelectric Ceramics		
20. ABSTRACT (Continue on reverse side if necessary and identify by block number) Experiments have been performed in ferroelectric ceramics on interface elastic wave guidance, laser probing of elastic vibration distributions, elastic attenuation, and the properties of counterpoled plates. —		

I. Introduction

During the past year, our attention has turned to the experimental aspects of creating domain walls (in our case, transition zones between regions of opposite polarity in piezoelectric ceramics), as well as the excitation and measurement of acoustic waves along these walls. We have conducted various poling experiments, and have successfully manufactured transition zones in ceramics of various types and thicknesses. In addition, we have investigated methods of directly measuring the polarization profile in these transition zones as a means of corroborating data obtained through measurements of acoustic waves traveling in the zones. As an aid in identifying suitable ceramics for reasonably lossless guided wave experiments, we have conducted attenuation measurements in various ceramics, among them, a special electrostrictive ceramic, PMN, supplied to us by Dr. L. E. Cross and coworkers at the Materials Research Laboratory at the Pennsylvania State University. Finally, as a means of experimentally verifying the theoretical results on wave guiding presented in last year's report, we have begun working on the application of a surface scanning heterodyne laser probe to the measurement of acoustic field distributions in differentially poled ceramic plates.

II. Waveguide Experiments

As a first attempt to observe the type of wave propagation believed to exist along domain walls, we constructed a simple model of a domain wall by bonding, edge to edge, two uniformly poled PZT-8 ceramic plates oriented with their polarizations normal to the plate surfaces and anti-parallel with respect to each other (Fig. 1). The transducers that launched and received the waves were designed to operate at a wavelength of approximately three times the plate thickness (large enough to insure that higher order plate modes would not interfere with the experiment). Tone bursts at various frequencies were used to excite two input transducers, one located on the interface and the other a few millimeters off the interface, as shown in Fig. 1. Acoustic waves excited on and off the interface by these two transducers were received by similar output transducers. Measurements of pulse delay from input to output were made in an attempt to locate a conspicuously slow wave. The evidence obtained tentatively demonstrated the existence of a slower wave, but a definite interpretation was not possible because of the coexistence of unwanted modes of vibration. In other words, it appeared that an interface wave had been weakly excited by the transducer located on the interface, but it was obscured by a stronger excitation of plate modes not confined to the interface. As a result, we embarked on a study of methods to efficiently launch domain wall waves (also referred to as interface waves).

In our last report, we made an extensive theoretical investigation of these interface waves. The wave we investigated had its particle motion along the polar axis, and propagated in the transverse plane normal to this

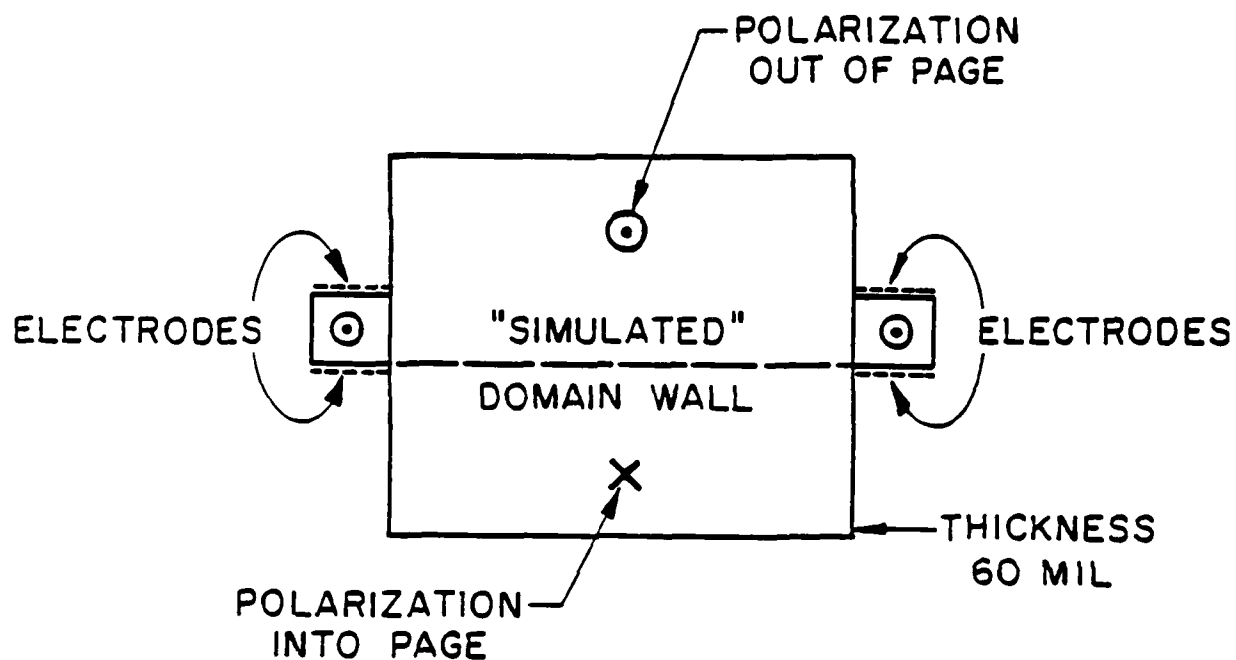


Fig. 1--PZT-8 ceramic structure for simulated domain wall wave experiment. The domain wall is simulated by bonding together two oppositely poled plates of ceramic, and acoustic waves can be launched into the structure by four surface wave transducers. One pair is used to conduct transmission measurements along the wall, and the other is used to excite waves off the wall.

axis (Fig. 2). The relevant piezoelectric coupling coefficient for exciting waves of this type is k_{15} , leading us to design the type of transducers shown in Fig. 3. These transducers consist of finger pairs parallel to the polar axis (z-axis) and periodic along the domain wall axis (y-axis). The electric fields arising from these transducers are oriented in the transverse plane, so that only the k_{15} coupled modes will be excited. As a test of the efficiency of these transducers in launching interface waves, two uniformly poled, thick PZT-8 bars were bonded together with their polar axes oriented anti-parallel to each other, as shown in Fig. 4. The interface formed by this bonding served as a model of the transition zone to be investigated in a differentially poled ceramic. We chose the thickness of the PZT bars to be large compared to an acoustic wavelength (the thickness of the structure was about 6λ). This choice was made to better model the infinite medium situation. We elected to concentrate on thick structures at first, since experiments involving these structures better lent themselves to interpretation based on an infinite medium theory. The finger pairs previously described were deposited along the edges of the two bars, coplanar with the interface, and oriented so as to launch waves along the interface (Fig. 4).

A structure having the same geometry and transducer placement as that in Fig. 4, but with two PZT bars poled in the same direction, was also made. Comparing this structure with parallel polarization to the other structure with anti-parallel polarization gives us a direct comparison of the effects of polarization reversal on wave propagation. Both pulse and cw transmission measurements are currently in progress on these samples, and preliminary results indicate a strong interface guidance in agreement with theoretical predictions.

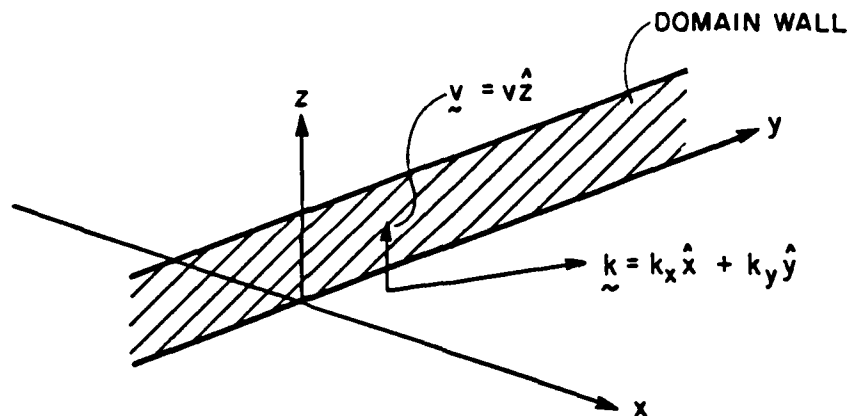
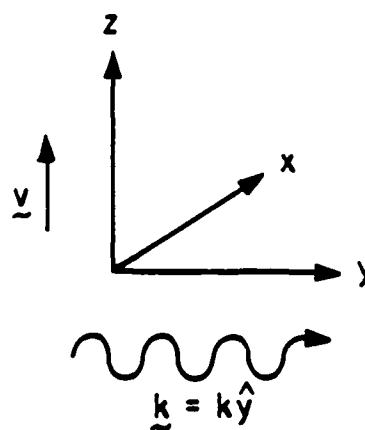
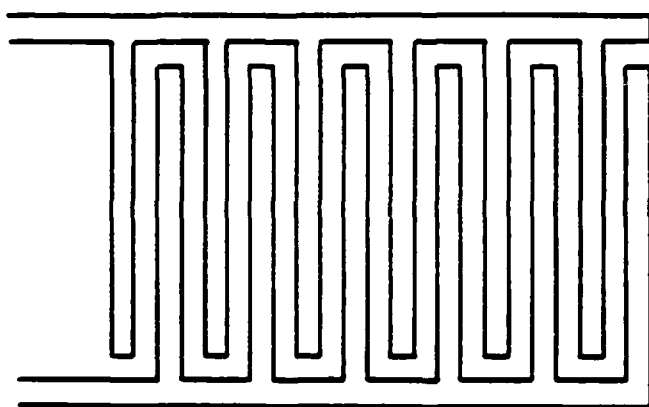


Fig. 2--Basic geometry for the study of shear-type domain wall waves in an infinite medium uniform in z .



E-FIELDS LIE IN xy -PLANE.
 PARTICLE MOTION POLARIZED
 ALONG z -AXIS.

Fig. 3--Finger pair transducer used in the excitation of shear-type domain wall waves.

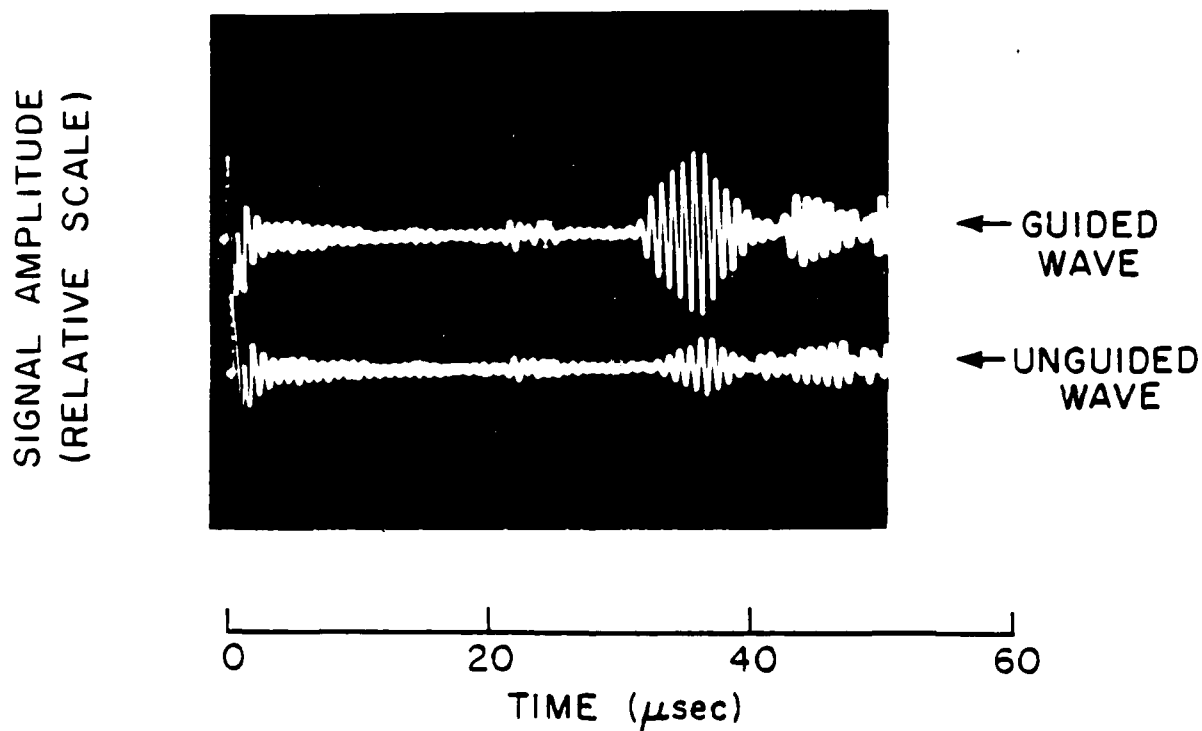
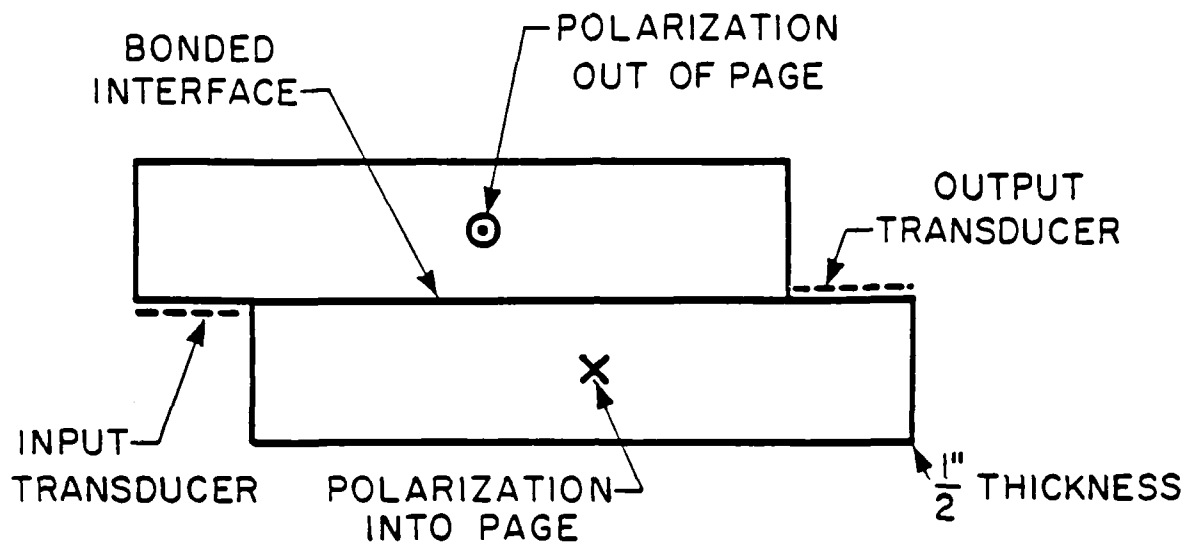


Fig. 1--Top: Improved experimental set-up for domain wall wave transmission experiments.

Bottom: Pulse transmission measurements demonstrating wave guidance in this structure ($f = 1.15 \text{ MHz}$).

III. Laser Probe Experiments

We are also interested in measuring the elastic vibration profile of a guided interface wave. This profile gives a measure of how tightly bound the guided wave is to the interface, as well as a way to recognize the presence of higher order guided modes characterized by different spatial distributions. As a means of measuring this vibration profile, we have begun implementing a heterodyne laser probe which scans along a polished surface and records the acoustic field amplitude at various points. Utilization of this technique requires that ceramic samples be polished to a highly reflective finish, which we have succeeded in doing for PZT-8 and PZT-5A. Our waveguide structures are polished in such a manner as to implement eventual laser scanning measurements.

This laser probe is based on the system described by Ash and coworkers.¹ As shown in Fig. 5, a laser beam at frequency ω_0 is directed into an acoustic Bragg cell driven at frequency ω_B . The acoustic wave set up in the Bragg cell serves as a "moving diffraction grating", which splits the incoming beam into an unchanged zeroth order beam with an array of frequency shifted, diffracted side lobes. This zeroth order beam reflects from the vibrating surface and returns along the same path into the Bragg cell, where it once again interacts with the acoustic wave of Bragg frequency ω_B . The "down-shifted" or $\omega_0 - \omega_B$ component of this returning "signal" beam is intercepted by a small mirror, and directed into a photodiode. Meanwhile, the "up-shifted" or $\omega_0 + \omega_B$ component of the original laser beam has also been reflected back upon itself, and returns through the Bragg cell. From the

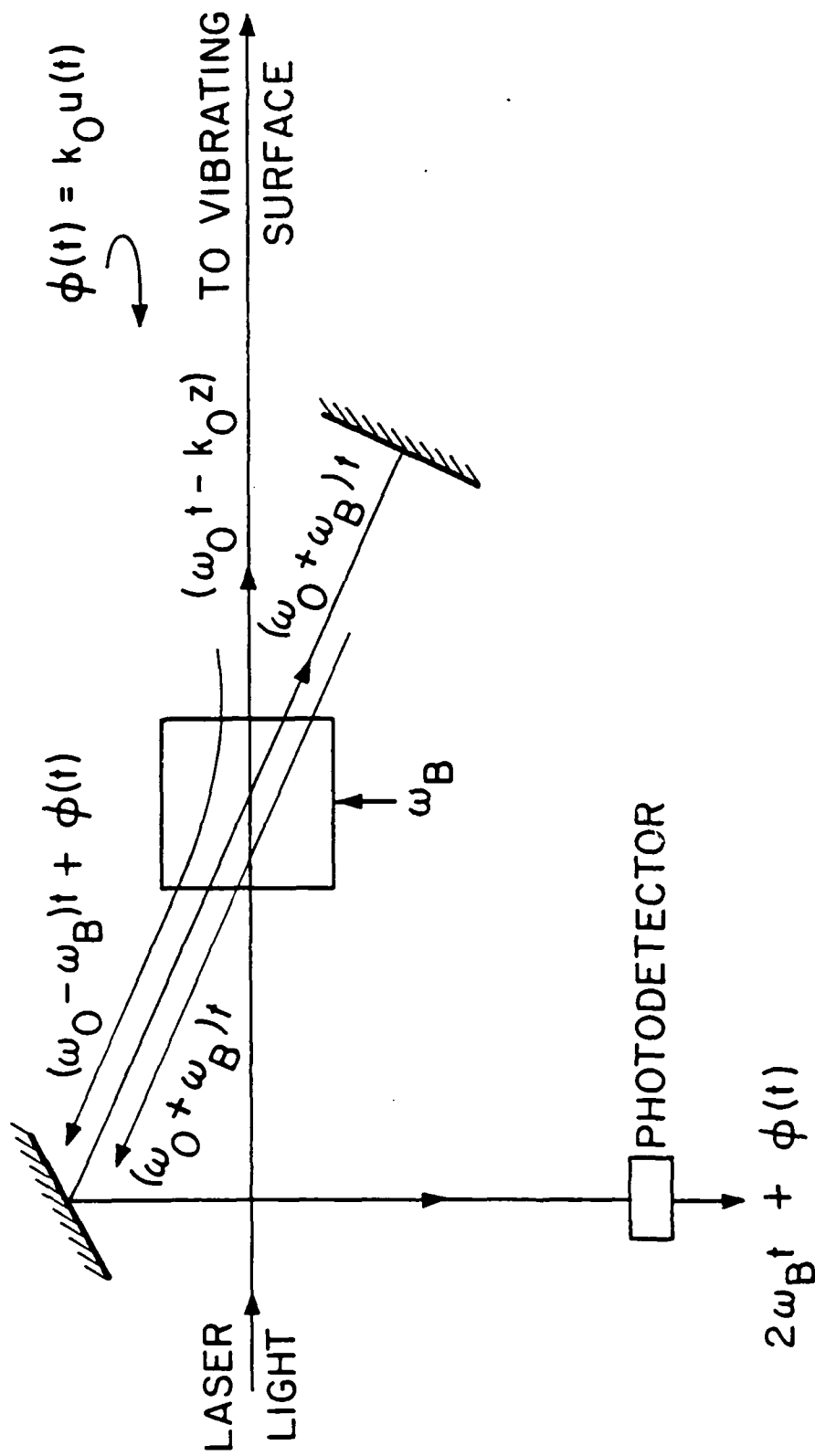


Fig. 5--Optics used in the heterodyne laser probe for the detection of acoustic vibrations in a polished ceramic.

geometry of Bragg diffraction, the zeroeth order of this returning $\omega_0 + \omega_B$ "reference" beam will be colinear with the $\omega_0 - \omega_B$ component of the returning "signal" beam, and will mix with this beam at the photodiode. If the signal beam path length and the reference beam path length are adjusted to be nearly equal (within the laser coherence length) the photodiode output is a signal of the form $\cos [2\omega_B t + \varphi(t)]$, where $\varphi(t)$ is the time-varying difference in optical path lengths between the reference and signal beam caused by the motion of the vibrating surface. In fact, $\varphi(t)$ is linearly proportional to the normal elastic vibration amplitude, d , at the polished surface, and can be written as:

$$\varphi(t) = 2d \cos \omega_A t \quad (1)$$

where ω_A is the acoustic frequency at which the surface is vibrating.

The photodiode signal is demodulated by the electronics depicted in Fig. 6. In our case, the discriminator is a sharp bandpass filter operated about a frequency where the filter's transfer function $H(f)$ is a rapidly varying linear function of frequency. This operating point f_0 is chosen such that the slope of the transfer function dH/df evaluated at this point is very large, and higher derivatives $d^{(n)}H/df^{(n)}$ are as small as possible. Therefore, an expansion of the transfer function $H(f)$ about the carrier frequency f_0 yields:

$$H(f) \approx H(f_0) + \left. \frac{dH}{df} \right|_{f=f_0} (f - f_0) \quad (2)$$

Small deviations in f arising from the phase modulation in Eq. (1) will be "magnified" by the steep slope of the transfer function, and appear as amplitude modulation on the output signal. This amplitude modulation envelope is

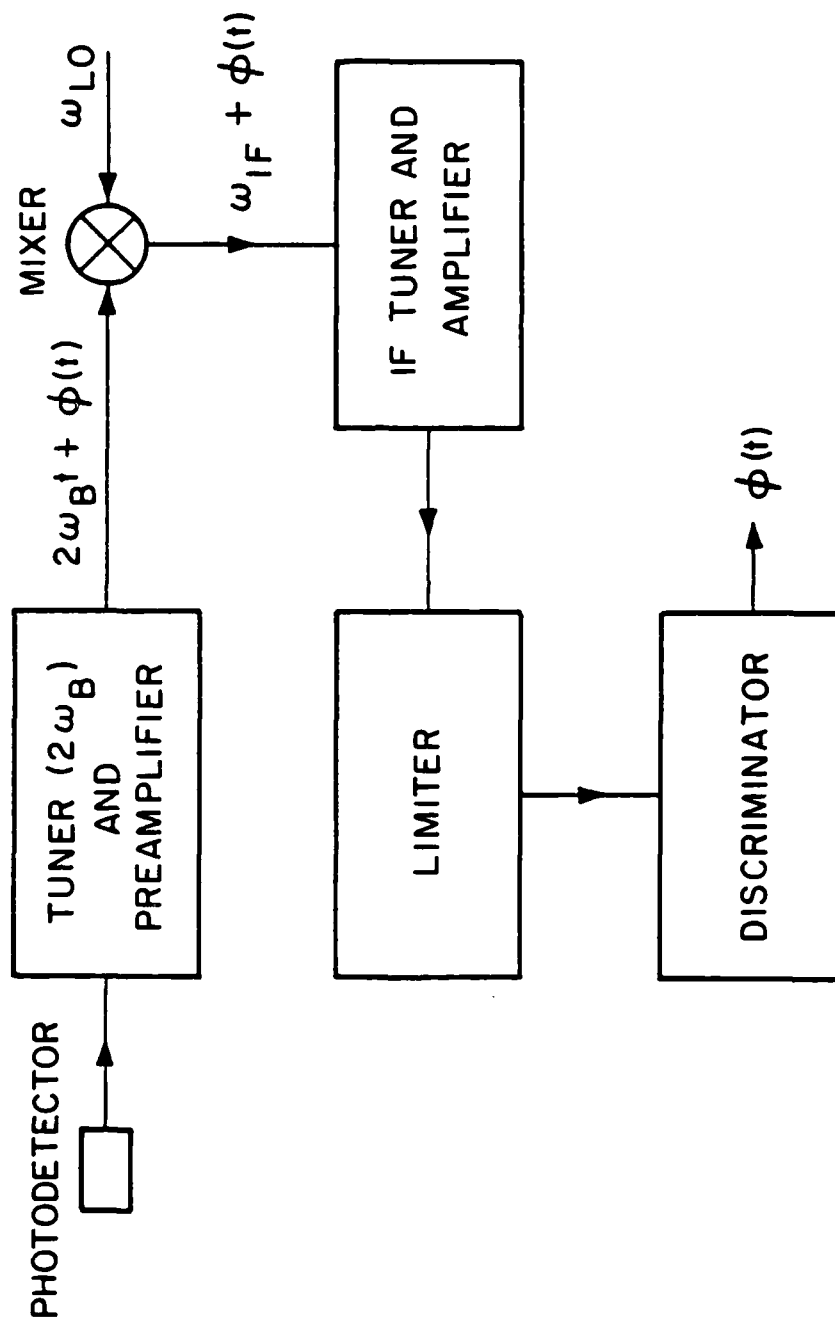


Fig. 6--Electronics for the heterodyne laser probe system.

then detected, and yields a signal proportional to the original phase modulation $\phi(t)$. From this, one obtains both amplitude and phase information about the acoustic wave propagating in the polished structure.

IV. Attenuation Measurements

In the past year, we have also been conducting attenuation measurements on various ceramics. These were made on PMN ceramics $[\text{Pb}_3(\text{MgNb}_2)\text{O}_3]$ as well as on some commercially available PZT ceramics. In attempting to characterize these materials by their attenuation factor, we employed two experimental methods. The first was the buffer rod method, wherein a buffer plate is sandwiched between a transducer and the sample whose loss is to be measured. The transducer is then excited with a tone burst, and the echoes from the buffer/sample interface and the sample's backface are measured. The first echo measured the pulse reflected back to the transducer from the buffer/sample interface. The amplitude of this pulse echo is directly proportional to the reflection coefficient R at the interface. The second echo arises from the pulse which travels into the sample, reflects off the backface, and returns through the interface to the transducer. This pulse echo contains information about both the round-trip loss in the sample $e^{-2\alpha L}$, and the reflection coefficient R . The third echo measured represents a pulse entering the sample, making two round-trips in the sample, and returning to the transducer. Manipulating the amplitudes of these three quantities, we can solve for the reflection coefficient R and the sample's attenuation constant α . In this manner, we measured attenuation constants for various PZT ceramics with pulses propagating along the polar axis.

Unfortunately, the buffer rod method yielded results which were difficult to reproduce and not very reliable. For PZT-8 at 5 MHz, we obtained values for attenuation ranging from 1.2 to 5.0 dB/inch. For the $\text{Pb}_3(\text{MgNb}_2)\text{O}_3$

at this frequency, we obtained much higher losses, ranging from 13 to 20 dB/inch. From our studies, it appeared that the measured value of loss depended on the positioning of the transducer and buffer on the sample. In addition, our values for loss seemed to be unusually high when materials with tabulated attenuation coefficients (like aluminum) were tested. One possible explanation is that the transducers we were using were too large for the specimens we were studying. Since the plates we studied had face dimensions only slightly larger than the transducers themselves, the acoustic waves interacted with the plate edges, complicating the propagation behavior and preventing a simple interpretation based on plane wave propagation.

The second method employed was superior in many respects. The ceramics to be studied were immersed in a water bath and a broadband piston transducer excited a water wave normally incident on the ceramic face. The transducer in this experiment was $1/8$ " in diameter, for samples of approximate dimensions $1" \times 1/2"$, so that the size problems encountered in the previous method were avoided. The transducer in this case was driven by a voltage "spike", so that a broad band of frequency components were excited. The ceramic sample is first aligned so that the received signal returning from the front face of the sample is maximized (corresponding to normal incidence of the acoustic wave). Then a pulse echo measurement is made, and the amplitudes as a function of time of the first three pulse echoes are stored in a computer. Numerical Fourier transforms of these stored signals are then computed, giving us the frequency spectrum of each pulse. From these spectra we then determine the material loss as a function of frequency. We wish to acknowledge the assistance of F. Stanke of the Ginzton Laboratory in performing these experiments.

Two examples of the loss curves obtained from this method are shown in Figs. 7 and 8. Figure 7 demonstrates the frequency dependence of acoustic attenuation in $\text{Pb}_3(\text{MgNb}_2)\text{O}_3$. This material is an electrostrictive ceramic and is isotropic in the absence of an applied electric field. As expected, the loss in this material is significantly larger than the loss of a wave propagating along the polar axis of PZT-8. The frequency dependence of the loss factor in the PMN ceramic appears to be roughly f^2 in a range between 4 and 12 MHz. In measuring the loss of this material, we noticed a slight anisotropy which introduced some beam walk-off and made accurate results difficult to obtain.

The anisotropy in the PZT-8 presented no problem, since the polar axis was aligned normal to the plate's faces. Therefore, a normally incident beam on the front face would propagate into the ceramic along the polar axis, and walk-off does not occur. The attenuation measured in PZT-8 was very low and between 12 and 24 MHz fitted the curve $0.00332 f^{2.45}$. The source of this unusual frequency dependence is not clearly understood at this time.

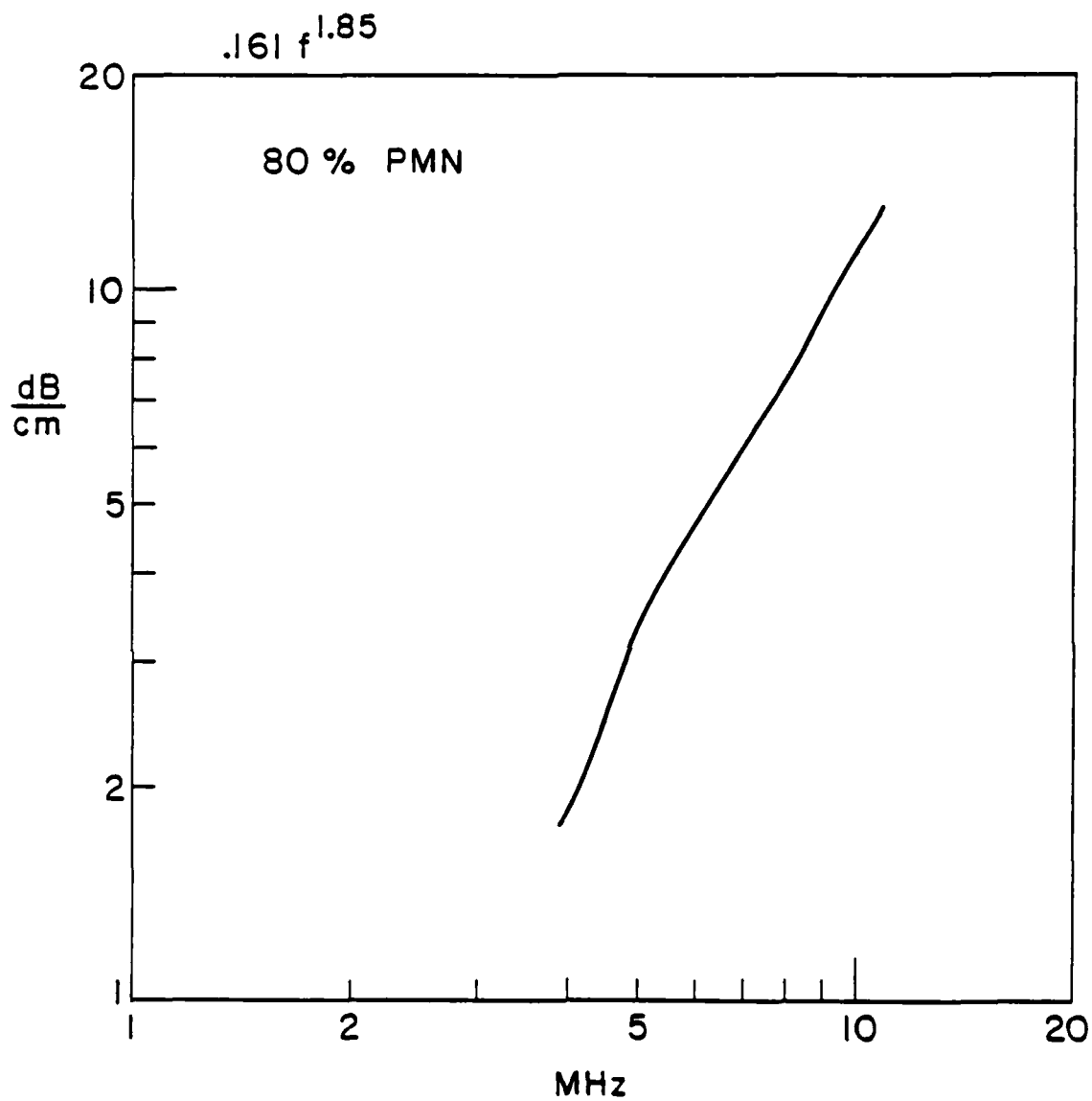


Fig. 7--Acoustic attenuation vs. frequency in $\text{Pb}_3(\text{MgNb}_2)\text{O}_7$ electrostrictive ceramic. The data closely fits the curve $.161 f^{1.85}$.

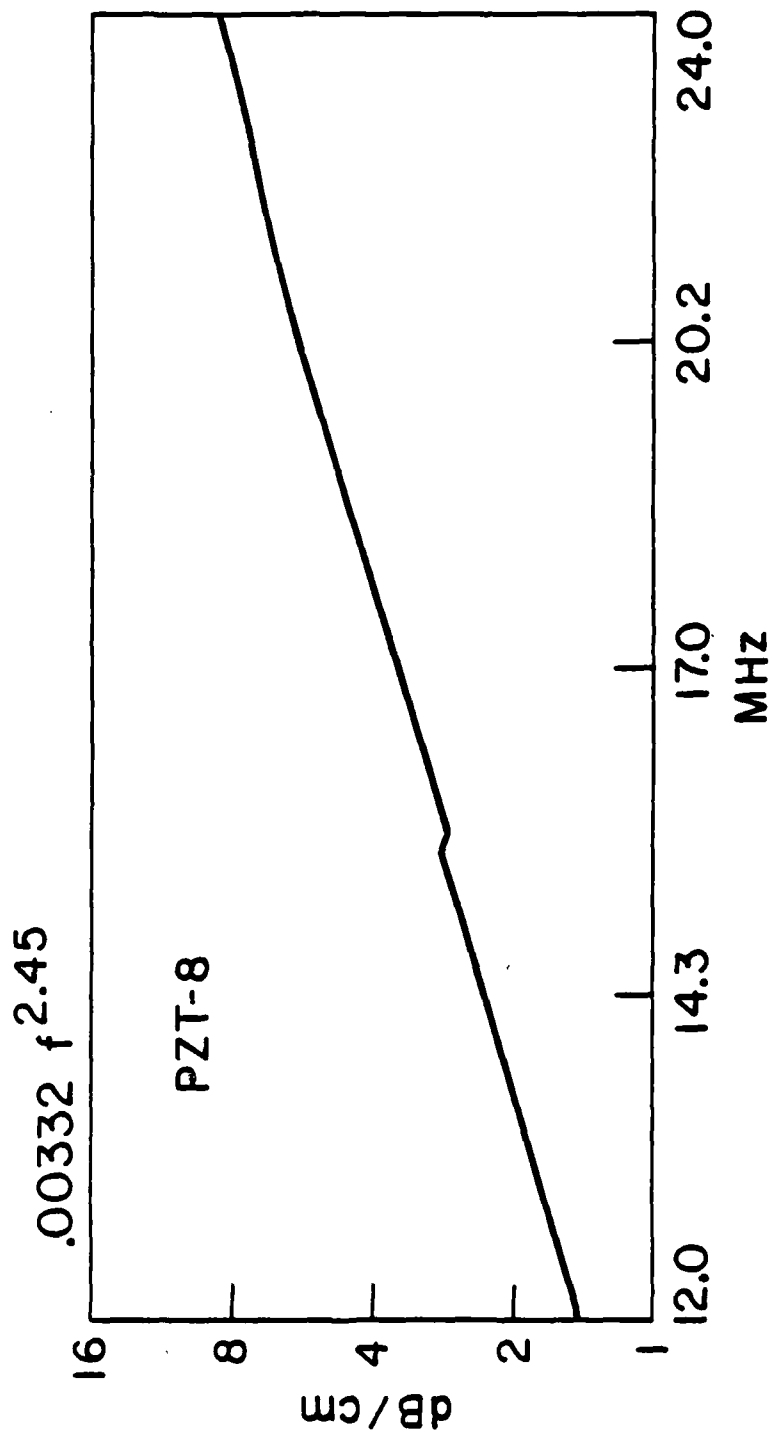


Fig. 8--Acoustic attenuation vs. frequency in PZT-8 (note log-log scale).
The data closely fits the curve $.00332 f^{2.45}$.

V. Poling and Counterpoling Experiments

This past year, we embarked on a study of poling procedures with the eventual aim of fabricating transition zones in piezoelectric ceramics. We have successfully poled and counterpoled various types of PZT ceramic plates having thicknesses up to 1/4". In our poling experiments, the samples are immersed in a bath of peanut oil heated to 140°C - 150°C. Poling fields in the range 50 kV/inch to 60 kV/inch are applied to perform the required re-alignment of electric dipoles. When poling and counterpoling was performed at these temperatures and field strengths, we found that most of the domain realignment in the ceramics we measured occurred within the first minute of poling. After five minutes of subsequent poling, there was only a small increase in the ceramic polarization.

To measure these levels of polarization at various points on the ceramic plate, we designed a pressure point scanning probe (Fig. 9). A rod with a small steel ball glued to one end was centrally mounted on the cone of a vibrating loudspeaker so that speaker motions would drive the rod like a piston. The ceramic to be measured was clamped on a brass ground plate and the loudspeaker was positioned so that the rod and steel ball remained pressed against the ceramic during a complete cycle of speaker motion. Hence, the ball exerted a time-varying pressure on a small region and a piezoelectric current proportional to the net polarization in that region was generated. A DC signal proportional to the amplitude of this piezoelectric current was displayed on the Y axis of our oscilloscope, and the probe's position on the X axis. By scanning the probe across the ceramic sample, a profile of spontaneous polarization versus position was obtained.

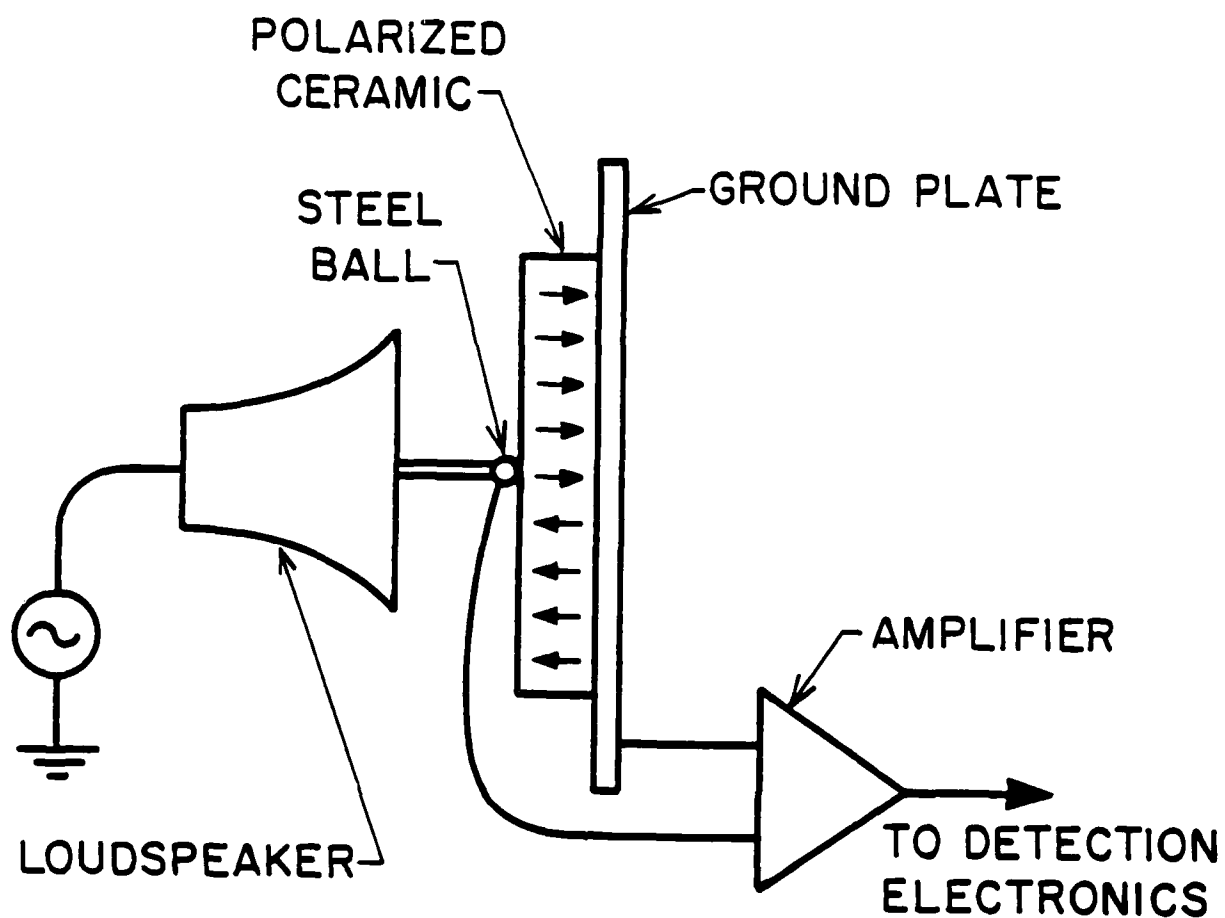
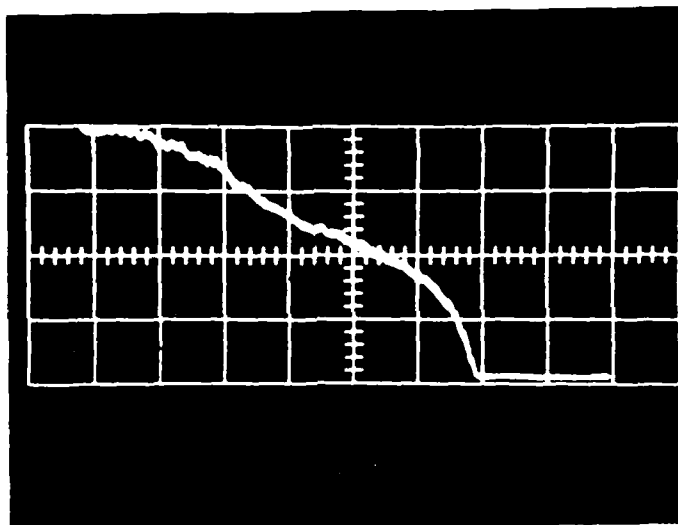


Fig. 9--Loudspeaker scanning probe for measurement of remanent polarization in a piezoelectric ceramic.

We used this poling probe to measure both the degree to which a sample was poled and the uniformity of poling across the sample. The probe was also used to measure the polarization profile in a differentially poled ceramic. A typical profile for a 3 mm thick piece of differentially poled PZT-8 is shown in Fig. 10. This sample was made by uniformly poling a piece of fully electroded PZT-8, then replacing one of the electrodes with a half electrode and reverse poling the region under the half electrode. Afterwards, the face with the half electrode was ground flat, and the piece was scanned with the loudspeaker probe. As is demonstrated in Fig. 10, the ceramic has "stored" a polarization profile which indicates the original position of the counterpoling electrode (on the right). The ceramic under this electrode is seen to be very well counterpoled. In addition, depoling has occurred in the region not under the counterpoling electrode, creating a transition zone of width greater than 1.5 mm or one-half of the plate thickness. The propagation of acoustic waves in transition zones of this nature is governed by a theory which takes into account not only the width of the zone, but the manner in which the ceramic's material constants vary in the zone. We devised a theory of this sort for the infinite medium case (included in the January 1980 Annual Report) and demonstrated the existence of higher order waveguide modes which can propagate in transition zones of finite width. We are planning to expand the theory to include semi-infinite half spaces and infinite plates.

Two possible factors which contribute to the large width of these transition zones are: (1) fringing fields extending from the edges of the counterpoling electrode, which partially depole nearby regions, and (2) internal rearrangement of the grains in the transition zone, resulting from transient changes in the strain state of the ceramic as it is counterpoled. We believe

POLARIZATION PROFILE



POSITION (.38 mm/DIV)

Fig. 13--Polarization profile of a differentially poled piece of PZT-5 measured by the loudspeaker probe.

that it is possible to minimize the effect of the fringing fields by carefully controlling the poling time and applied field. Since the fringing fields are weaker than the fields between the electrodes, domain alignment in these fringe regions will require more time than alignment between the electrodes. Hence, it is important that we remove poling fields as soon as possible, keeping the effects of fringing fields to a minimum.

The effect of depoling strain on the creation of transition zones has been observed and is currently being investigated. The axial strain on a poled ceramic can be on the order of 0.3% in relation to the depoled state. These enormous strains clearly play a role in physically deforming a differentially poled ceramic. It is possible that the electrical depoling observed to occur in transition zones is a consequence of a large elastic strain destroying the grain alignment of a previously poled region. In the coming year, we plan to attempt a separation of this strain depoling effect from the fringing field effect previously described.

VI. Conclusion

We have conducted waveguide experiments using a ceramic model of a thin domain wall which demonstrate the existence of guided acoustic waves traveling along the interface. In the coming year, we will use a heterodyne laser probe to measure the elastic vibration amplitude and the dispersion relation of these waves. We are also researching simple but effective ways to launch waves of this nature by experimenting with new transducer designs.

In the past year, we have also manufactured actual transition zones in various piezoelectric ceramics. We have developed a pressure probe device to measure polarization profile in these differentially poled ceramics, and have observed large ceramic deformation in the regions near the transition zone. In the coming year, we hope to implement a laser technique to simultaneously measure polarization profile and surface deformation in these ceramics. We will also carry out waveguiding experiments on these differentially poled ceramics, and correlate acoustic data obtained from these experiments with simultaneously measured polarization profiles. Using these techniques we hope to begin a characterization of different ceramics based on the physics of their transition zones.

VII. References

1. R. M. De La Rue, R. F. Humphreys, I. M. Mason, and E. A. Ash, Proc. IEEE 119, 117-126 (1972).

VIII. Presentations

B. A. Auld, "Wave Propagation and Resonance in Piezoelectric Materials," presented at the Invited Session on One Hundred Years of Piezoelectricity, 100th Meeting of the Acoustical Society of America, Los Angeles, November 1980.

IX. Visits

B. A. Auld attended the Materials Research Laboratory review presentation on Targetted Basic Studies of Ferroelectric and Ferroelastic Materials for Piezoelectric Transducer Applications, October 1980.

DATE
FILMED
—8